

TWENTYFIFTH EUROPEAN ROTORCRAFT FORUM

Paper n° G22

**COAXIAL HELICOPTER ROTOR
DESIGN & AEROMECHANICS**

BY

**Boris N. Bourtsev, Sergey V. Selemenev, Victor P. Vagis
KAMOV Company, Moscow Region, Russia**

**SEPTEMBER 14 – 16 , 1999
R O M E
I T A L Y**

**ASSOCIAZIONE INDUSTRIE PER L'AEROSPAZIO, I SISTEMI E LA DIFESA
ASSOCIAZIONE ITALIANA DI AERONAUTICA ED ASTRONAUTICA**

Introduction

The advanced technology is based on mathematical simulation (software), on a model testing, on a flight tests and on an experience of helicopter development, on the new developed materials.

The Fig.1A & Fig.1B show basic parameters of coaxial KAMOV's helicopters.

1. Coaxial rotor mathematical simulation & physical experiments

The survey of the theoretical and experimental coaxial rotor aerodynamic research published by Coleman, C.P. [4] and by Bourtsev, B.N. [9,10].

The paper [9,10] presents the results of figure of merit analysis for single and coaxial main rotors at hover as well as for a helicopter with a tail rotor and a coaxial helicopter. The analysis has been performed using a simple physical model based on the results of numerical simulation, wind tunnel tests and full scale flight tests.

It is demonstrated [9,10] that a characteristic feature of coaxial main rotor is a high aerodynamic perfection at hover caused by an additional amount of air being sucked in by the lower main rotor (Fig.2). The coaxial rotor at hover demonstrates a 13% larger figure of merit value in comparison with a single rotor unbalanced by torque (Fig.2). Absence of tail rotor power losses provides a 20% larger figure of merit for a coaxial helicopter as a rotorcraft (Fig.2, Fig.4). Fig.3 presents the coaxial rotor figure of merit. These results were obtained by measuring in full scale flight test at hover.

Full-scale flight investigation of a Ka-32 coaxial helicopter tip vortex wake structure was successfully completed [5,6]. A smoke visualization method was applied using blades smoke generators installed. A tip vortex wake was visualized in hover, at low flight speeds and medium flight speeds (Fig.3, Fig.5). A specific dimensionless number has been adopted to determine inductive velocities and flight speeds related to an ideal inductive velocity in hover (Fig.5). The wake form was determined and the tip vortex velocities were measured in hover. The tip vortex vertical velocities turned out to be less than the inductive velocity of the ideal rotor in hover. The measured wake contractions were equal to 0.85R for the upper rotor and 0.91R for the lower rotor (Fig.3).

The tip vortex coaxial rotor wake was visualized in a forward flight. In the rotor front part the free tip vortices were positioned above the tip path planes. That flat part of a free wake could extend along the rotor up to 3/4 of its radius (Fig.5).

2. Basic design solutions and aeroelastic phenomena

It is very important to have a substantiation of aeromechanical phenomena. This is feasible given adequate simulation making possible to explain and forecast:

- natural frequencies of structures;
- loads & deformation;
- aeroelastic stability limits: stall flutter, transonic flutter, ground resonance;
- helicopter performance & maneuverability.

KAMOV Company has developed software to simulate a coaxial rotor aeroelasticity [1,2,3,8,9,10]. Aeroelastic phenomena to be simulated are shown in the Fig.6 as (1-7) lines in the following way:

- (1) - system of equations of coaxial rotor blades motion ;
- (2) - elastic model of coaxial rotor control linkage (boundary data);
- (3) - model of coaxial rotor vortex wake;
- (4,5,6) - steady and unsteady aerodynamic airfoils data;
- (7) - elastic / mass / geometry data of the upper / lower rotor blades and of the hubs.

The lines (1-8) in Fig.6 show functional capabilities of the software. Columns (1-5) conform to versions of the software . Both steady flight modes and manoeuvres of the helicopter are simulated .

Based on experience of KAMOV Company new key design approaches regarding the coaxial rotors of the Ka-50 helicopter were developed.

The blade aerofoiles were developed by TsAGI for the Ka-50, Ka-115, Ka-226 helicopter specially (Fig.7). Optimal combination of $C_L, C_D, C_M(\alpha, M)$ characteristics was a necessary condition to achieve:

- high G-load factor & stall limit ;
- acceptable margin of flutter speed ;
- low loads of rotor & linkage ;
- low vibration level ;
- high helicopter performance.

Blade sweep tips developed by KAMOV Company affords for the same purposes.

Usage of all key approaches regarding rotors becomes an sufficient condition to achieve high performance of the rotor system and therefore of the helicopter as whole.

3. KAMOV's Key Technologies

3.1 Fiberglass & fiber graphite rotor blades

In the end - 1950's KAMOV Company designed, built and tested fiberglass rotor blades. In 1965 first production fiberglass rotor blades were successfully flown on the KAMOV Ka-15 helicopter. In 1967 first production fiberglass rotor blades were successfully flown on the KAMOV Ka-26 helicopter. In the end 1970's the graphite & glass fiber rotor blades were successfully produced by KAMOV Company.

The graphite fibers had potential specific stiffness values which six times those of current aircraft materials. This proved to be highly significant in addressing elastic stability and aeroelastic design problems.

The combination of glass and graphite fibers resulted in excellent, benign failure modes and provided aerodynamics, structures and dynamic engineers.

Ka-50 helicopter advanced rotors geometry is:

- special airfoil;
- blade optimal twist;
- blade swept tip (Fig.7).

All KAMOV's blades fitted with electrothermal de-icing system.

3.2 Advanced rotor blade retention technology

All before Ka-50 KAMOV's helicopters had full articulated rotor hubs. Ka-32 helicopter has metal hubs, mechanical & elastomeric bearings & dampers (Fig.8).

Ka-50 helicopter has metal and composite hubs, elastomeric bearing & damper, flex element for pitch, flapping and lag (Fig.8).

3.3 Rotor control linkage

The rotor control linkage parameters determine a flap-lag-pitch motion and a motion stability of rotor blades (Fig.6, Fig.8, Fig.9).

The mathematical model of coaxial rotor control linkage was developed by KAMOV Company [1]. This math model is used for control linkage design and for frequency & stability analysis.

The control linkage elasticity matrix-functions was measured for full scale coaxial helicopters of four types.

The analysis of the experimental results determined to develop a control linkage mathematical model and a adequate formula

for the "approximation-calculation" of the matrix-function elements. With the help of this formula the rigidity characteristics of the control linkage aggregates were determined without their physical measuring for coaxial helicopters of four types. It is demonstrated that the eigenvectors of the elasticity matrix are actually torsional modes of the six blades on the control linkage and the eigenvalues are actually linkage "dynamic elasticities" of the corresponding mode which are usually measured in a different way - that is by the linkage frequency testing. The study results are illustrated on Fig.9 [1].

4. The basic design aeromechanic & aeroelastic problems of coaxial rotor helicopter have been developed and key technologies have been achieved

4.1 KAMOV Company experience concentrated in the Ka-50 attack helicopter

Acceptable margin of flutter speed and stall flutter speed of the Ka-50 helicopter were substantiated by mathematical simulation and validated by flight test results (Fig.10). Flight tests results are shown by ($V_{TAS} - \omega R$) relation in Fig.10. A part of flight test points is given in the frame, namely the following range: from $V_{TAS} \sim 300 \text{ km/h}$ to $V_{NE} = 350 \text{ km/h}$, till $V_{TAS} = 390 \text{ km/h}$. Flutter is non-existent in restricted range of calculated curve what is verified by flight test results. Calculated curve presents that there is a flutter speed margin of about 50 km/h (Fig.10).

Vibration level of the coaxial helicopter have been discussed in paper [2]. The alternating forces apply to hubs of the upper/lower rotors and excite airframe vibration. Configuration of the Ka-50 helicopter rotors affords applying of minimal alternating forces to the airframe. In this case vibration level of the airframe is minimal too.

Vibration level is not in excess of $0.01g$ in main flight modes. Rotor pendulum and anti-resonant isolation system are not used. The example shown on Fig.11 [2].

Special task for the coaxial helicopter is making a provision for the acceptable lower-to-upper rotor blade tips clearances. As a task of aeromechanics it is analogous with a task to provide the blade tips-to-tail boom clearance of the helicopters with the tail rotor.

KAMOV Company applies at analysis both calculation methods and flight tests [3, 8]. The clearances are measured with the help of optic devices at each of 6 crossing points when the upper blades are arranged above lower blades during their relative rotation with doubled angular speed.

The mechanics can be outlined as following (Fig.12). The planes of the upper / lower rotor blade tips are in parallel at hover. Their clearance is even more than a clearance between rotor hubs.

At forward flight variable azimuthal airloads occur in the rotor disk, that results in flapping motion. Because of this , planes of the upper / lower rotor blade tips are inclined to equal angles in flight direction (forward / backward).

In lateral direction (viewed along flight direction) the planes of blade tips are inclined to each other because of counter-rotation of the rotors (Fig.12).

The upper-to-lower tips clearances on one disk side decreases and increases on the opposite one. In lateral direction an inclination angle of blade tip planes is approximately equal to blade tip flapping angle (to the left / to the right) and depends on flight mode (Fig.12). As known from aeromechanics, there are relations between blade flapping angle and the rotor parameters, especially to Lock number, blade geometrical twist angle and blade/control linkage torsional stiffness.

Calculation and flight test results show the values of coaxial rotor parameters mentioned above which ensure acceptable safety clearance.

Fig.12 demonstrates measured blade tip flapping angles made during flight tests of Ka-50 helicopter and comparison with calculation data .

Ka-50 helicopter generalised measurement results for the forward flight and manoeuvres are presented in the Fig.12, Fig.13.

The acceptable upper-to-lower rotor blade tips clearances were substantiated by mathematical simulation and validated by flight tests results for all approved envelope of manoeuvres.

The acceptable lower rotor blades to tail boom clearances were validated .

4.2 Ka-50 helicopter maneuverability features

Load factor / speed envelope was substantiated and validated by Ka-50 flight test results:

- within operational limitations (pitch, roll, rotor speed, rotor loads,...);
- within special aerobatic limitations.

A part of flight test points is illustrated by the Fig.13 :

at $3.5 > \text{g-factor} > 2$ & at $\text{g-factor} \approx 0$.

Each point corresponds to one of the performed manoeuvres . The most part of them are shown at the Fig.13 No established limitations have been exceeded .

Fig.13 also shows the test flight results of Tiger's helicopter [13].

The table on the Fig.14 presents parameters of manoeuvres within special limitations for aerobatic flights. It is notable in this case parameters of "flat turn" and pull-out from the skewed loop at $\text{g-factor} = 3.5$.

4.3 The means of aerobatic flight monitoring and analysis

The NSTAR software was created to provide processing and analysis of Ka-50 helicopter test flight data. Using records made by aircraft test instrumentation the NSTAR software makes possible to restore the flying path and to calculate flight parameter additional values [14].

NSTAR software is comparable both with test flight record system and with standard record system. NSTAR results are used for the following purposes:

- analysis of actions , assistance in pilot training;
- examination for critical parameter limits;
- as input data for simulation.

Fig.14 presents an example for skewed loop path recovery.

5. Conclusions

5.1 The basic aeromechanic & aeroelastic problems of a coaxial rotor helicopter have been developed and Key Technology have been achieved.

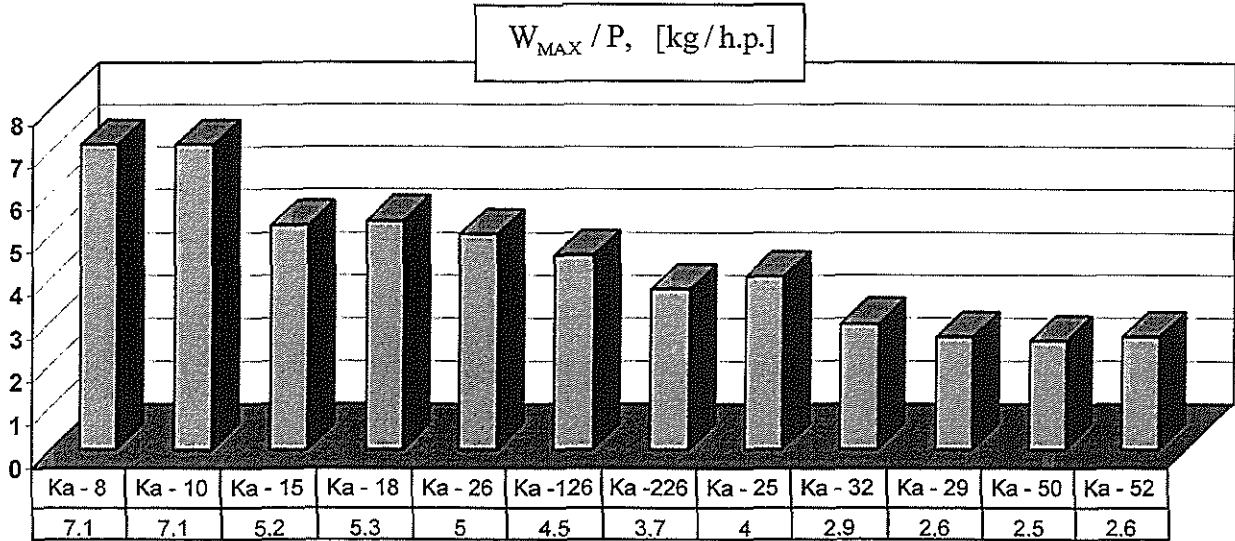
5.2 Key Technology determine the coaxial helicopter performance and manoeuvrability.

7. References

1. Bourtsev, B.N., "Aeroelasticity of Coaxial Helicopter Rotor", *Proceedings of 17th European Rotorcraft Forum*, Germany, Berlin, Sept. 1991.
2. Bourtsev, B.N., "The Coaxial Helicopter Vibration Reduction", *Proceedings of 18th European Rotorcraft Forum*, France, Avignon, Sept. 1992.
3. Bourtsev, B.N., Selemenev, S.V., "The Flap Motion and the Upper Rotor Blades to Lower Rotor Blades Clearance for the Coaxial Helicopters", *Proceedings of 19th European Rotorcraft Forum*, Italy, Como, 14 – 16 Sept. 1993.
4. Coleman, C.P., "A Survey of Theoretical and Experimental Coaxial Rotor Aerodynamic Research", *Proceedings of 19th European Rotorcraft Forum*, Italy, Como, 14 – 16 Sept. 1993.
5. Akimov, A.I., Butov, V.P., Bourtsev, B.N., Selemenev, S.V., "Flight Investigation of Coaxial Rotor Tip Vortex Structure", *ASH 50th Annual Forum Proceedings*, USA, Washington, DC, May 1994.
6. Акимов, А.И., Бутов, В.П., Бурцев, Б.Н., Селеменев, С.В., "Летные исследования и анализ вихревой структуры винтов соосного вертолета", *Российское Вертолетное Общество, Труды 1го Форума*, Россия, Москва, 20 – 21 Сентября 1994.
7. Bourtsev, B.N., Gubarev, B.A., "A Ka-115 Helicopter a New Development of KAMOV Company", *Proceedings of 22nd European Rotorcraft Forum*, Russia, Saint-Petersburg, 30 August – 1 Sept., 1995.
8. Bourtsev, B.N., Selemenev, S.V., "The Flap Motion and the Upper Rotor Blades to Lower Rotor Blades Clearance for the Coaxial Helicopters", *Journal of AHS*, No1, 1996.
9. Bourtsev, B.N., Kvokov, V.N., Vainstein, I.M., Petrosian, E.A., "Phenomenon of a Coaxial Helicopter High Figure of Merit at Hover", *Proceedings of 23rd European Rotorcraft Forum*, Germany, Dresden, 16 – 18 Sept. 1997.
10. Бурцев, Б.Н., Вайнштейн, И.М., Квоков, В.Н., Петросян, Э.А., "Феномен высокого коэффициента полезного действия соосных несущих винтов на режиме висения", *Российское Вертолетное Общество, Труды 3го Форума*, Россия, Москва, 24 – 25 Марта 1998.
11. Bourtsev, B.N., Koptseva, L.A., Animitsa, V.A., Nikolsky, A.A., "Ka-226 Helicopter Main Rotor – as a New Joint Development by KAMOV & TsAGI", *Aviation Prospects 2000, International Symposium*, Russia, Zhukovskiy Moscow Region, 19 – 24 August 1997.
12. Бурцев, Б.Н., Копцева, Л.А., Анимитца, В.А., Никольский, А.А., "Несущий винт вертолета Ка-226 – новая совместная разработка фирмы КАМОВ и ЦАГИ", *Российское Вертолетное Общество, Труды 3го Форума*, Россия, Москва, 24 – 25 Марта 1998.
13. Kurt Gotzfried, "Survey of Tiger Main Rotor Loads from Design to Flight Test", *Proceedings of 23rd European Rotorcraft Forum*, Germany, Dresden, 16 – 18 Sept. 1997.
14. Bourtsev, B.N., Guendline, L.J., Selemenev, S.V., "Method and Examples for Calculation of Flight Path and Parameters While Performing Aerobatics Maneuvers by the Ka-50 Helicopter based on Flight Data Recorded Information", *Proceedings of 24th European Rotorcraft Forum*, France, Marseilles, 15 – 17 Sept. 1998.
15. Mikheyev, S.V., Bourtsev, B.N., Selemenev, S.V., "Ka-50 Attack Helicopter Aerobic Flight", *Proceedings of 24th European Rotorcraft Forum*, France, Marseilles, 15 – 17 Sept. 1998.
16. Mikheyev, S.V., Bourtsev, B.N., Selemenev, S.V., "Ka-50 Attack Helicopter Aerobic Flight", *ASH 55th Annual Forum Proceedings*, Canada, Montreal, 25 – 27 May 1999.
17. Самохин, В.Ф., Ермилов, А.М., Котляр, А.Д., Бурцев, Б.Н., Селеменев, С.В., "Импульсное акустическое излучение вертолета соосной схемы при крейсерских скоростях полета", *Тезисы докладов на семинаре "Авиационная акустика"*, Россия, Дубна Московской области, 24 – 27 Мая 1999.

Basic Parameters of Coaxial KAMOV'S Helicopters

POWER LOADING



MAX SPEED

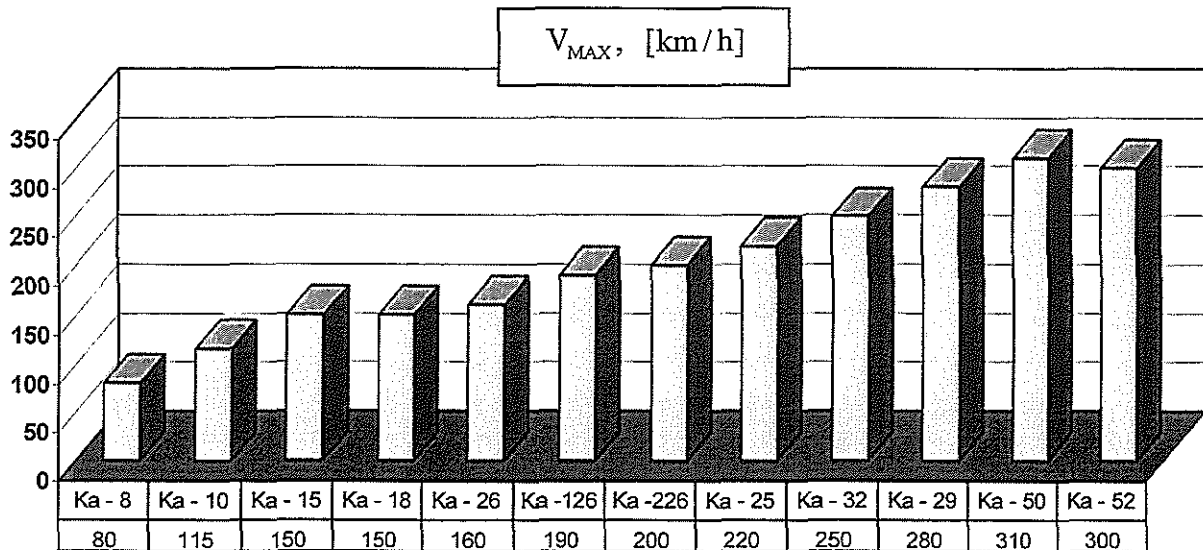
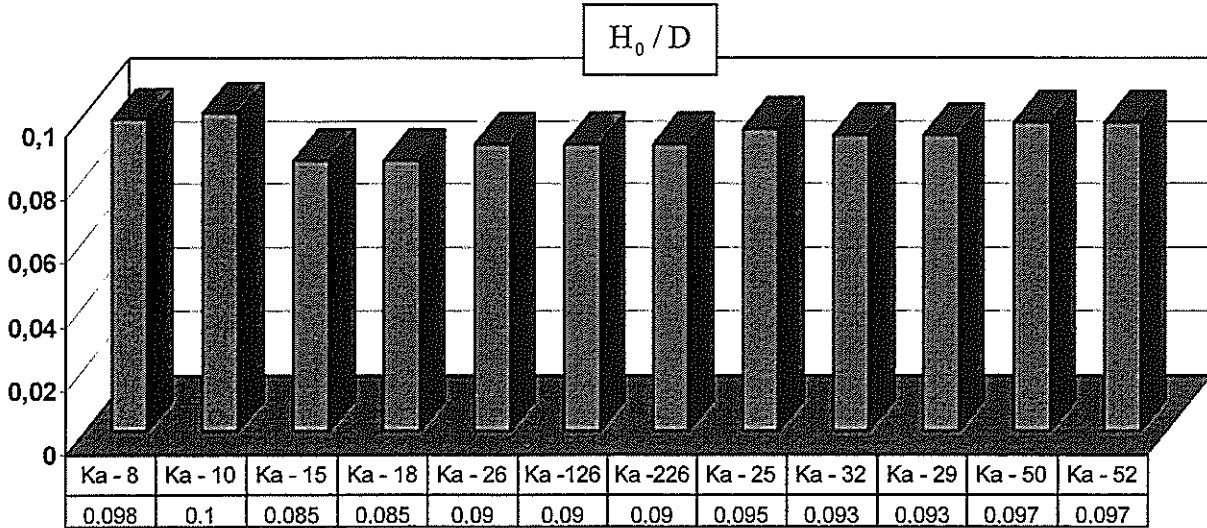


Fig.1A

Basic Parameters of Coaxial KAMOV'S Helicopters

RELATIVE HUB CLEARANCES



DISK LOADING

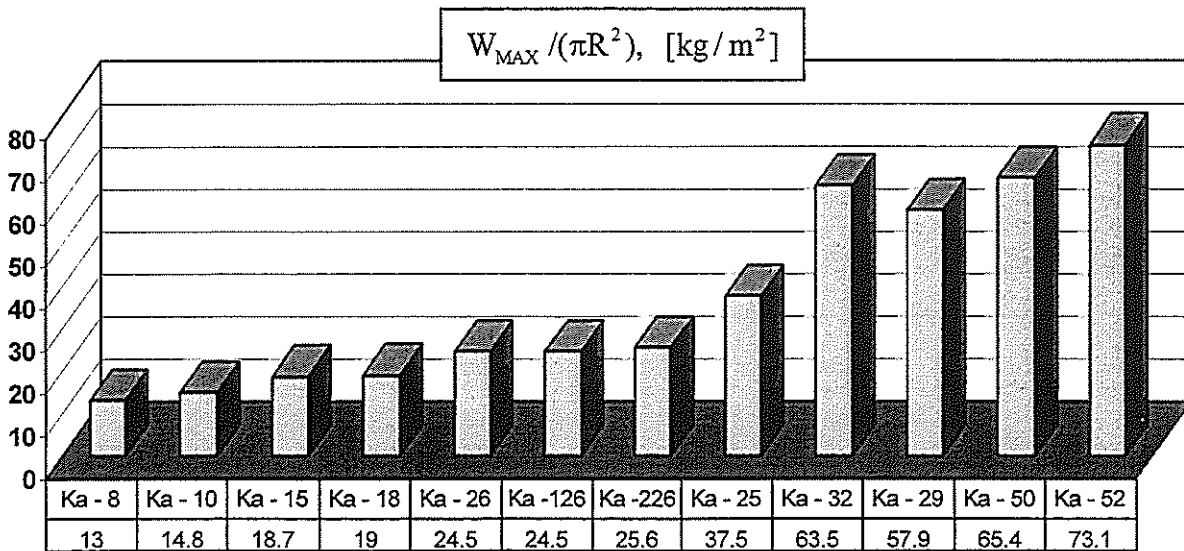
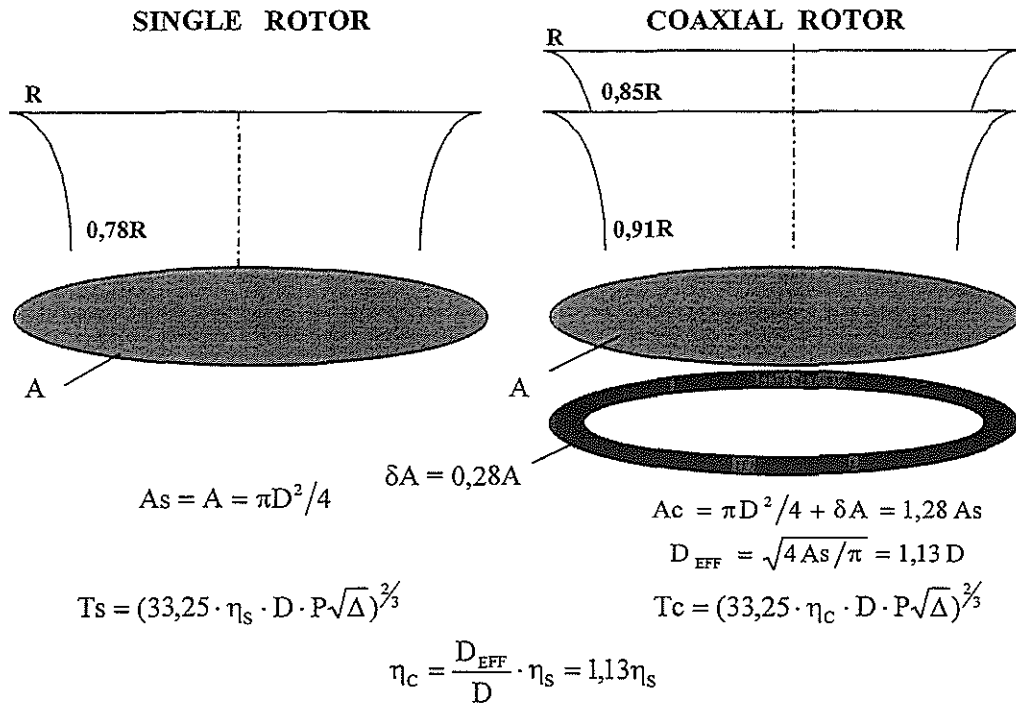


Fig.1B

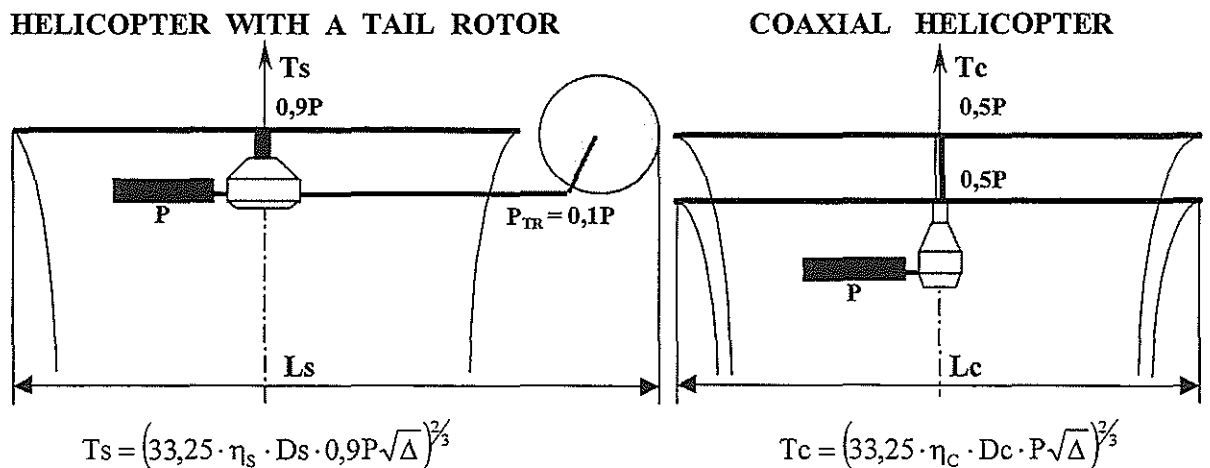
Single & Coaxial Rotors

active disk areas, effective diameters,
power & thrusts at hover



Single & Coaxial Rotor Helicopters

main rotor diameter, power & thrust at hover

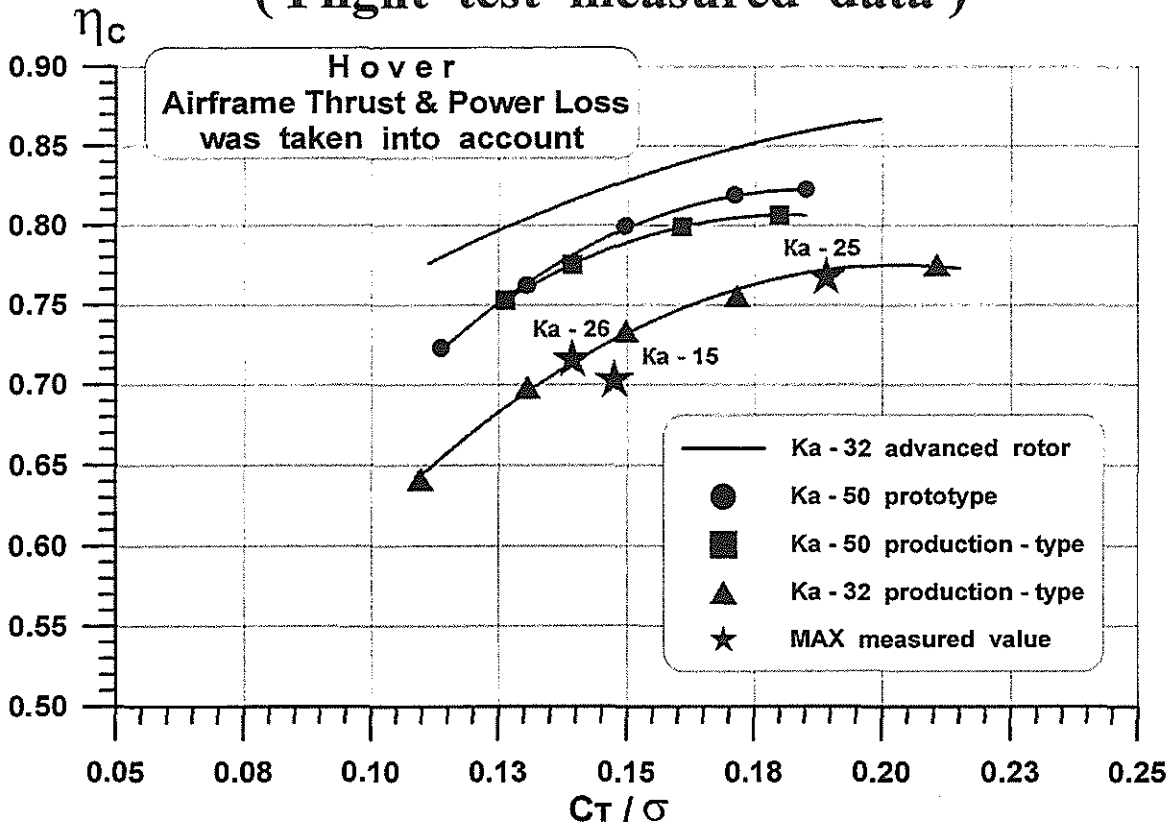


From $\eta_c / \eta_s = 1,13$ and $P_c = P_s = P$ and $P_{TR} = 0,1P$:

1. At $D_c = D_s$ the thrust ratio is $T_c / T_s = (1,13 / 0,9)^{2/3} = 1,16$;
2. At $T_s = T_c$ the diameter ratio is $D_s / D_c = 1,13 / 0,9 = 1,26$.

Fig.2

Figure of merit of coaxial rotors (Flight test measured data)



Wake form in hover & its approximation

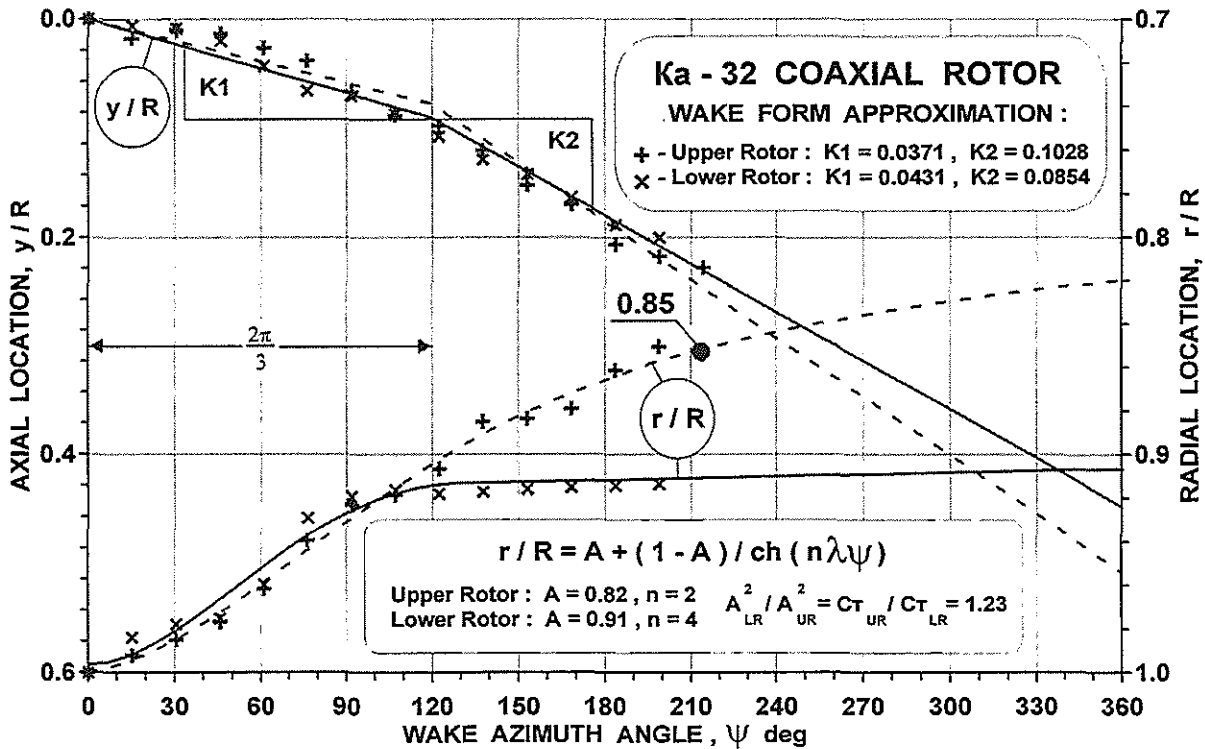


Fig.3

THE STATISTICAL CHART

Power Loading - Disk Loading - Design Figure of Merit of Coaxial Helicopters & Helicopters with a Tail Rotor

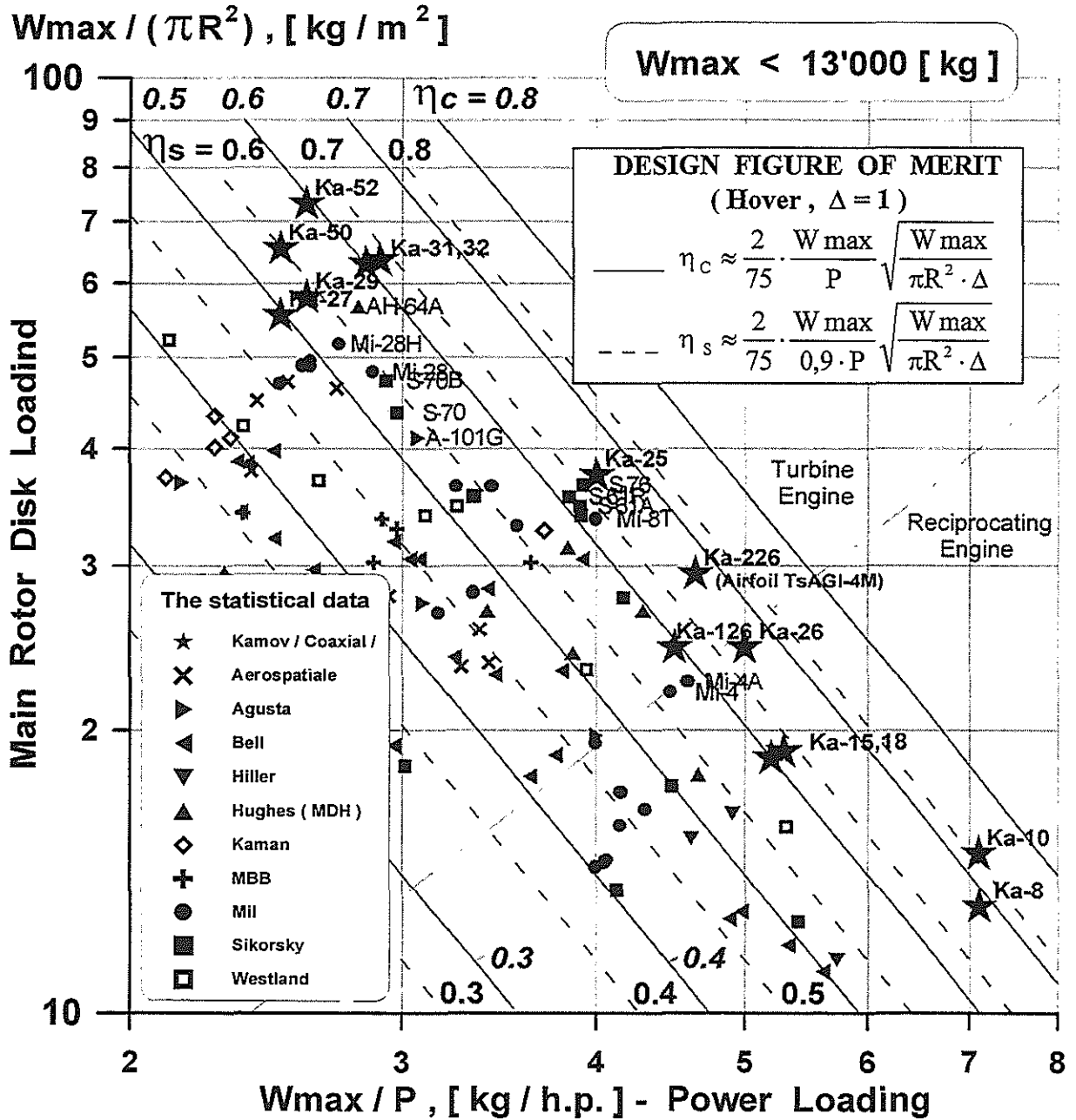


Fig.4

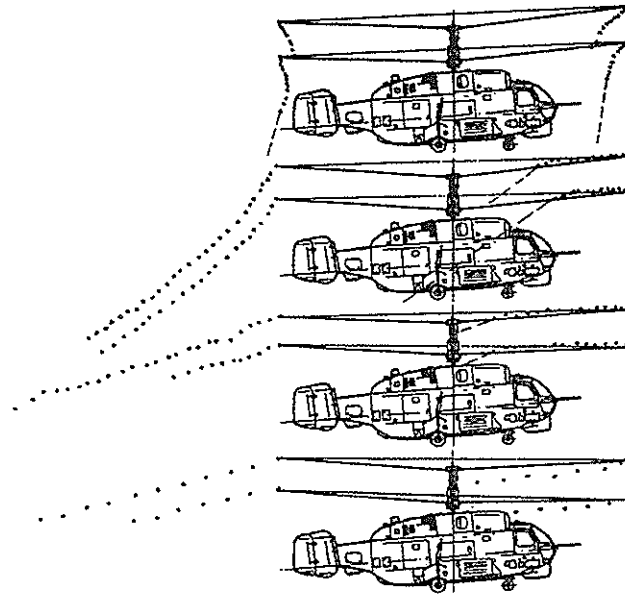
Coaxial Rotor Wake Side Views for Several Flight Speeds

$V_{TAS} = 5$ [km/h]

$V_{TAS} = 73$ [km/h]

$V_{TAS} = 138$ [km/h]

$V_{TAS} = 227$ [km/h]



Wake Front Boundary Longitudinal Position Versus Flight Speed

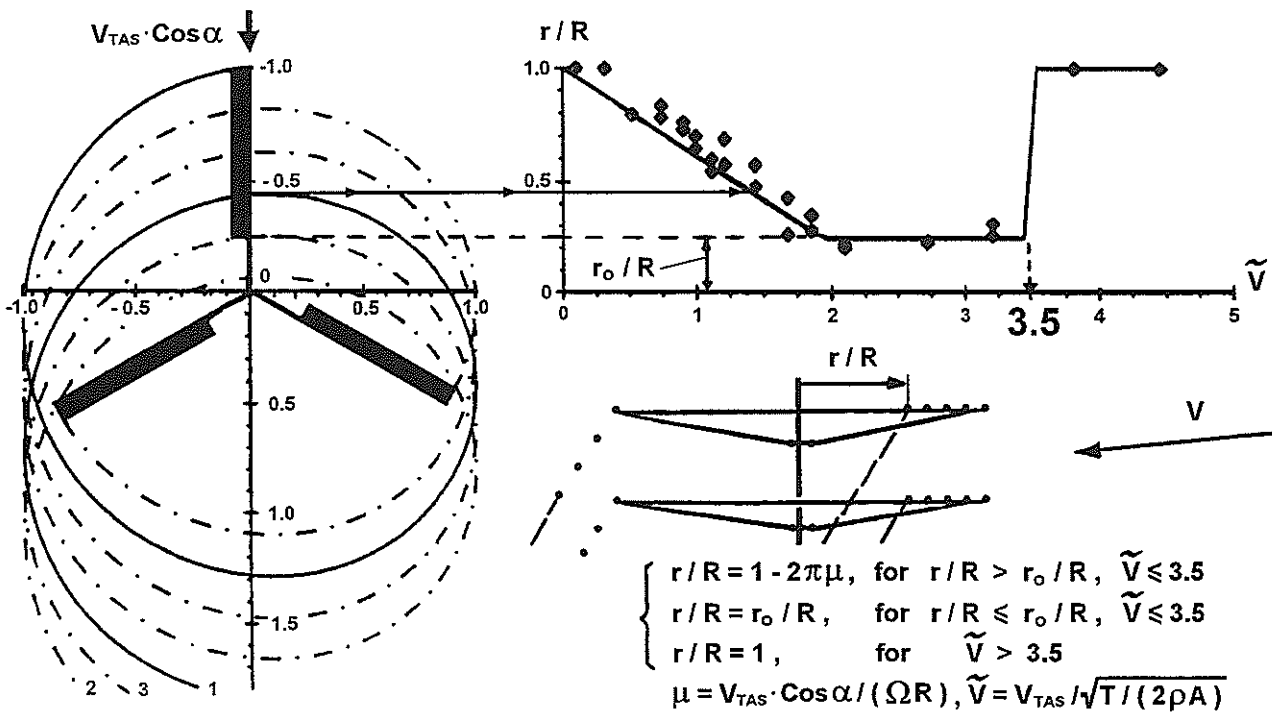


Fig.5

Simulated Aeroelastic Phenomena of Coaxial Rotor

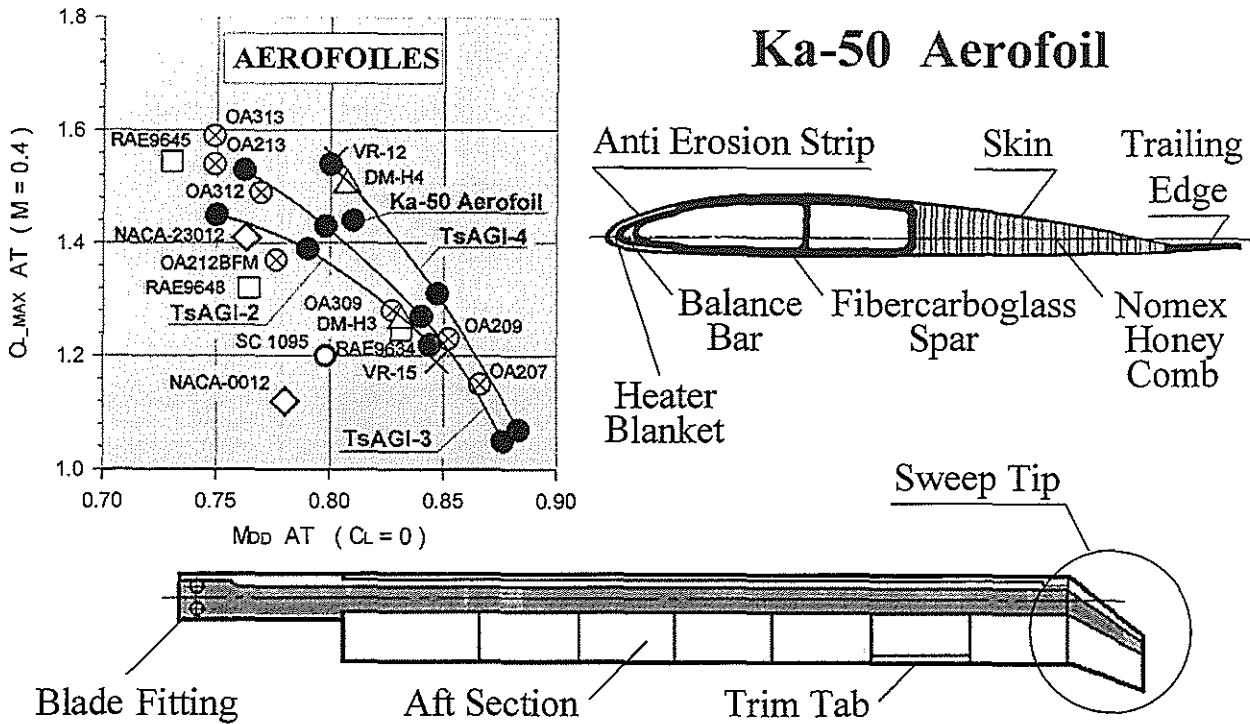
Simulated Phenomena		SIMULATION VERSION				
		ULISS-6	ULISS-1	ULMFE	FLUT	MFE
1	$EI_x (r/R, \omega t)$					
	$EI_y (r/R, \omega t)$	✓	✓			
	$GI_p (r/R, \omega t)$					
2	$\bar{\Phi}_0 = U_{ij} \times \bar{M}$	✓			✓	✓
3	$V_i (r/R, \psi)$	✓				
4	C_L, C_D, C_M $(\alpha, \dot{\alpha}, M, \dot{M})$	✓	✓	✓		
5	$C_{L,MAX}$ $(\alpha, \dot{\alpha}, M)$	✓	✓	✓		
6	Airfoil Aeroelastic Deformation	✓	✓	✓	✓	
7	Upper/Lower Rotor Data	✓	✓	✓	✓	✓

Analysis Results of Coaxial Rotor Aeroelastic Simulation

Analysis Results		SIMULATION VERSION				
		ULISS-6	ULISS-1	ULMFE	FLUT	MFE
1	Stall flutter boundary	Coaxial Rotors	Blade	Blade		
2	Bending moments, Pitch link loads, Actuator loads	Coaxial Rotors	Blade	Blade		
3	Elastic Deformations	Coaxial Rotors	Blade	Blade		
4	Alternate loads on Hubs	Coaxial Rotors				
5	Blade tips Clearances	Coaxial Rotors				
6	Flight test flutter	Coaxial Rotors	Blade	Blade		
7	Ground test flutter	Coaxial Rotors			Blade	
8	Natural frequencies			Blade		Blade

Fig.6

Blade Aerofoil Data



Aerodynamic moments of existing TsAGI-2, C_L TsAGI-4 airfoils & advanced TsAGI-4M airfoil

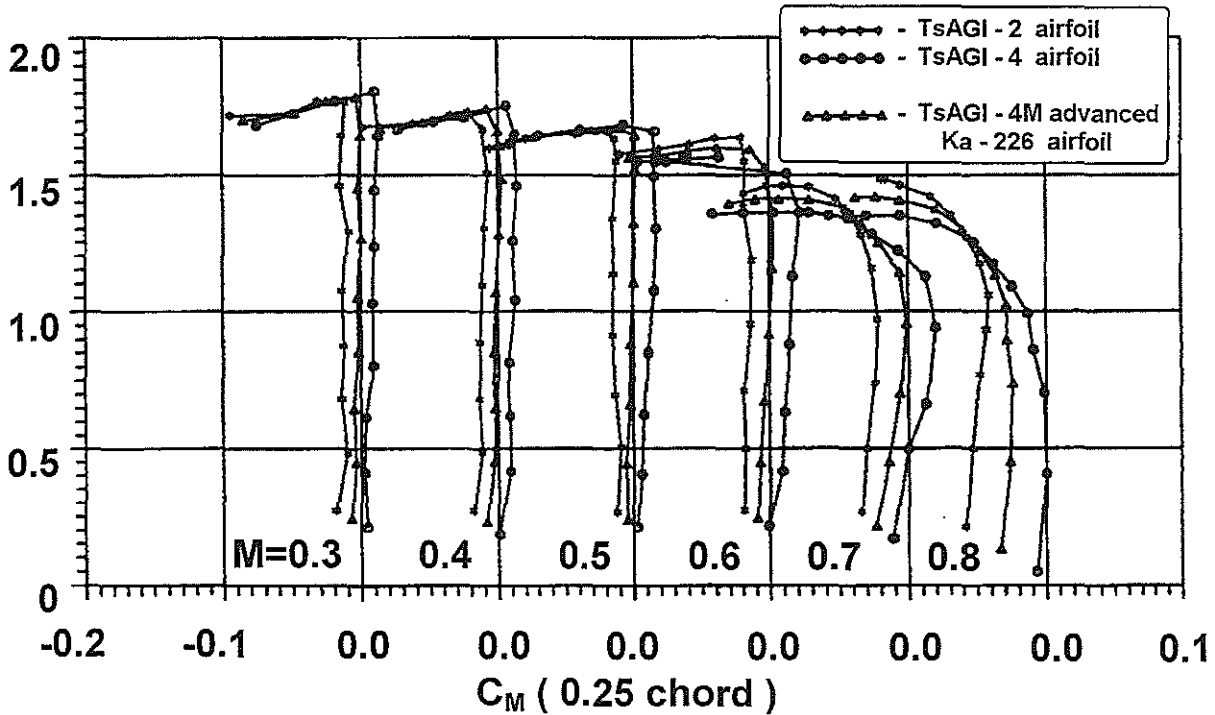
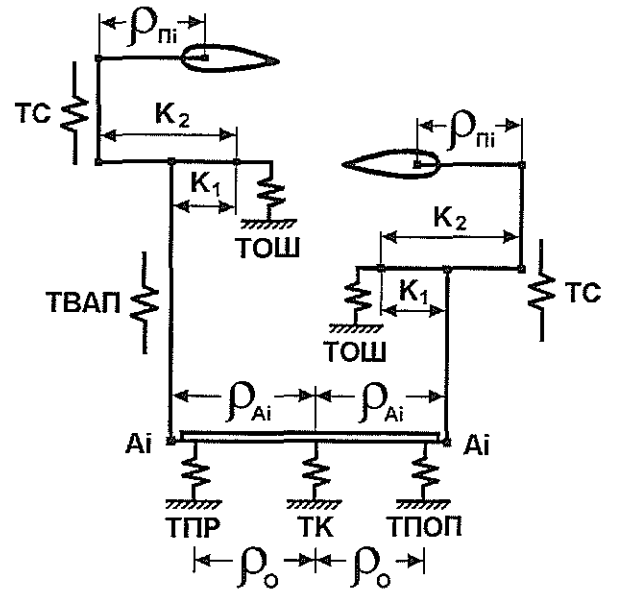
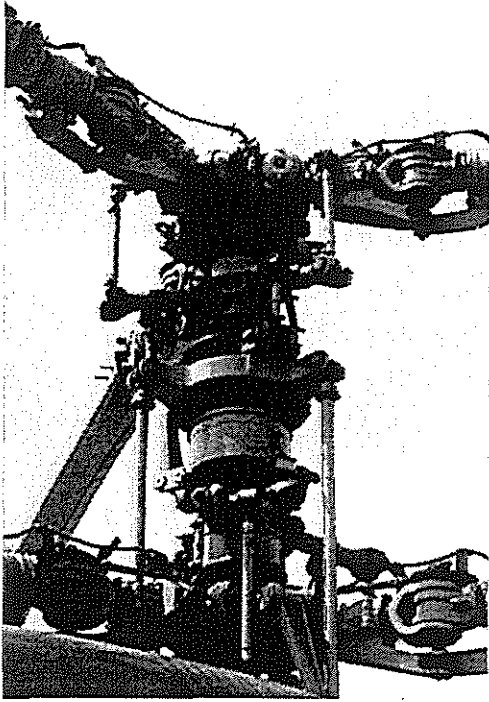


Fig.7

Ka-32 rotors control linkage model



Ka-50 rotors control linkage model

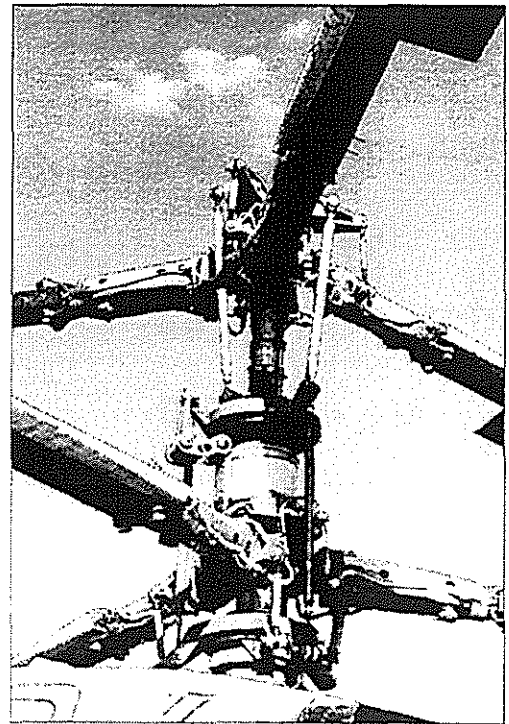
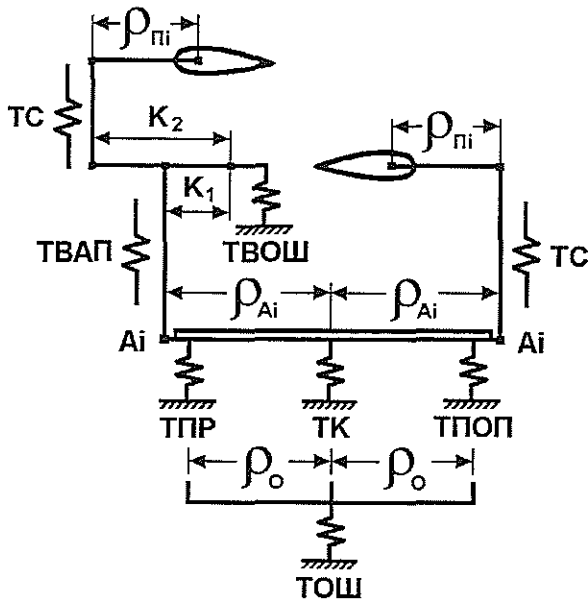
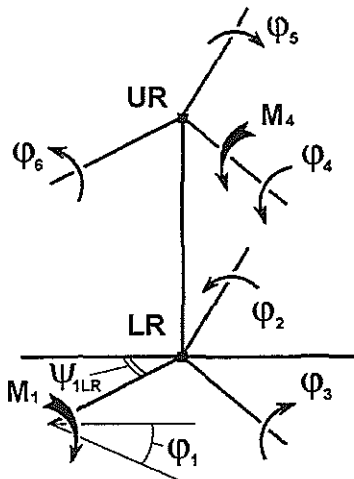
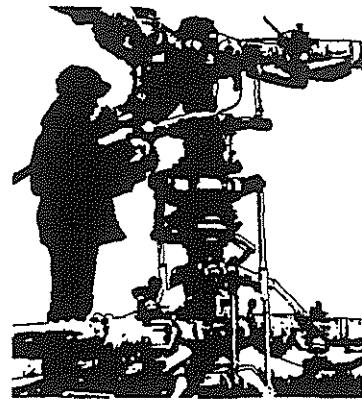


Fig.8

The scheme of experiment on determination of the control linkage elasticity matrix



$$\bar{\varphi} = \|\mathcal{G}_{I,J}\| \times \bar{M}$$

$$\begin{bmatrix} \bar{\varphi}_1 \\ \bar{\varphi}_2 \\ \bar{\varphi}_3 \\ \bar{\varphi}_4 \\ \bar{\varphi}_5 \\ \bar{\varphi}_6 \end{bmatrix} = \begin{bmatrix} \mathcal{G}_{11} & \mathcal{G}_{12} & \mathcal{G}_{13} & \mathcal{G}_{14} & \mathcal{G}_{15} & \mathcal{G}_{16} \\ \mathcal{G}_{21} & \mathcal{G}_{22} & \mathcal{G}_{23} & \mathcal{G}_{24} & \mathcal{G}_{25} & \mathcal{G}_{26} \\ \mathcal{G}_{31} & \mathcal{G}_{32} & \mathcal{G}_{33} & \mathcal{G}_{34} & \mathcal{G}_{35} & \mathcal{G}_{36} \\ \mathcal{G}_{41} & \mathcal{G}_{42} & \mathcal{G}_{43} & \mathcal{G}_{44} & \mathcal{G}_{45} & \mathcal{G}_{46} \\ \mathcal{G}_{51} & \mathcal{G}_{52} & \mathcal{G}_{53} & \mathcal{G}_{54} & \mathcal{G}_{55} & \mathcal{G}_{56} \\ \mathcal{G}_{61} & \mathcal{G}_{62} & \mathcal{G}_{63} & \mathcal{G}_{64} & \mathcal{G}_{65} & \mathcal{G}_{66} \end{bmatrix} \times \begin{bmatrix} M_1 \\ M_2 \\ M_3 \\ M_4 \\ M_5 \\ M_6 \end{bmatrix}$$

Elasticity matrix

APPROXIMATION: $\mathcal{G}_{I,J}(\psi_{1LR}) = f(TC, TK, T\Pi O\Pi, T\Pi P, TBA\Pi, TOIII, TBOIII, \psi_{1LR})$

CALCULATION:

$$\mathcal{G}_{I,J}(\psi_{1LR}) = \frac{KA\varphi_I}{\rho_{III}} \cdot \frac{KA\varphi_J}{\rho_{III}} \cdot \{TK \cdot [KA_I \cdot (\sin\varphi_I + \cos\varphi_I) - 1] \cdot [KA_J \cdot (\sin\varphi_J + \cos\varphi_J) - 1] +$$

$$+ KA_I \cdot KA_J \cdot (T\Pi O\Pi \cdot \cos\varphi_I \cdot \cos\varphi_J + T\Pi P \cdot \sin\varphi_I \cdot \sin\varphi_J)\} + TC + TBA\Pi + \mathcal{G}_{0,I,J};$$

$$\mathcal{G}_0 = \begin{bmatrix} TOIII & 2TOIII \\ 2TOIII & 4TOIII + TBOIII \end{bmatrix}; \varphi_I = \begin{cases} \psi_{1LR} + O\Pi - \frac{\pi}{2} - \frac{2\pi}{K}(I-1); & I=1, 2, \dots, K \\ 2\pi - (\psi_{1LR} + O\Pi + DFI) - \frac{\pi}{2} - \frac{2\pi}{K}(I-K-1); & I=K+1, \dots, 2K \end{cases}$$

Main rigidities of the elasticity matrix & dynamic rigidities obtained from frequency testing

$$\begin{cases} M\ddot{\varphi} + \mathcal{G}^{-1}\varphi = 0 \\ \varphi = u \cdot e^{ipt} \\ (\mathcal{G}M - E/P_K^2) \cdot u = 0 \\ P_K^2 = 1/(\lambda_K I) \end{cases}$$

MEASURED Ka - 32 ROTOR LINKAGE RIGIDITY \Rightarrow

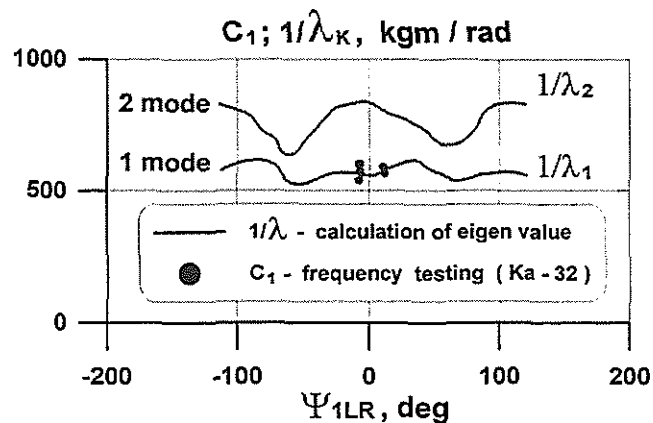
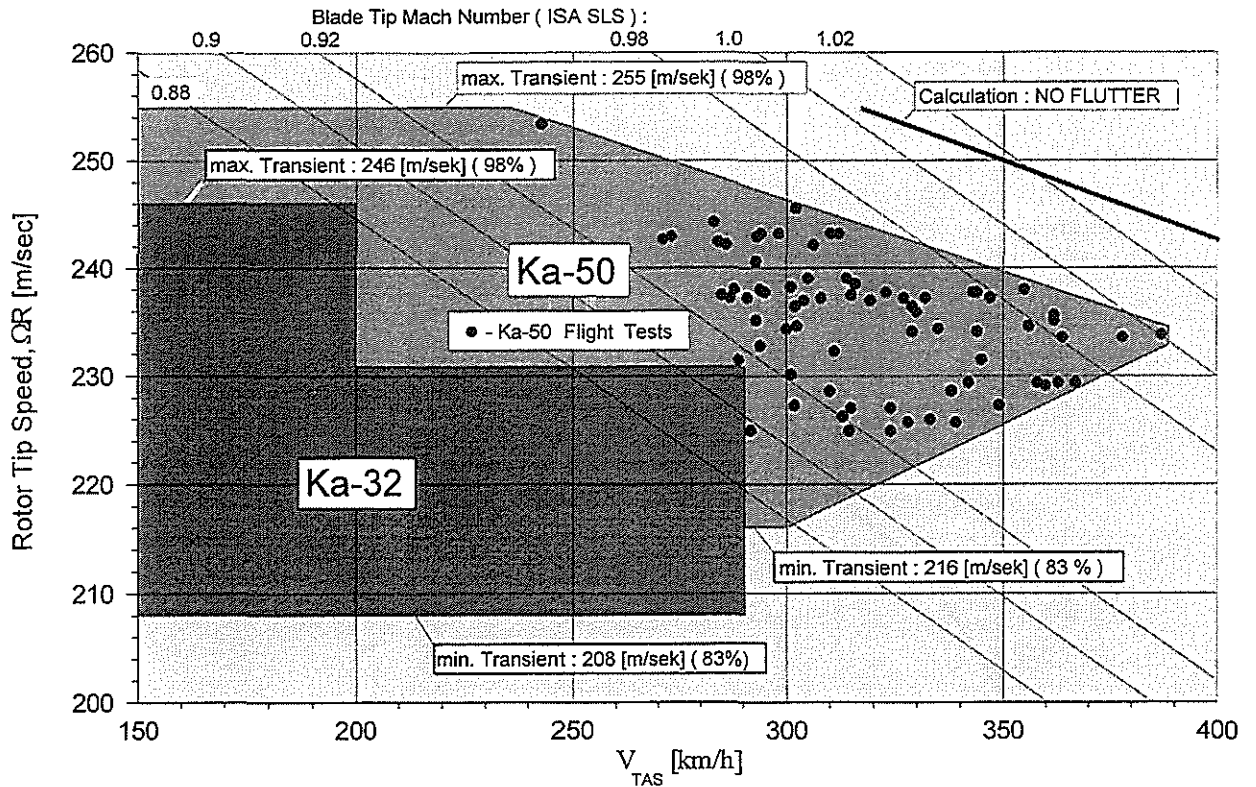


Fig.9

Demonstrated Rotor Speed Range



Stall Flutter Boundary

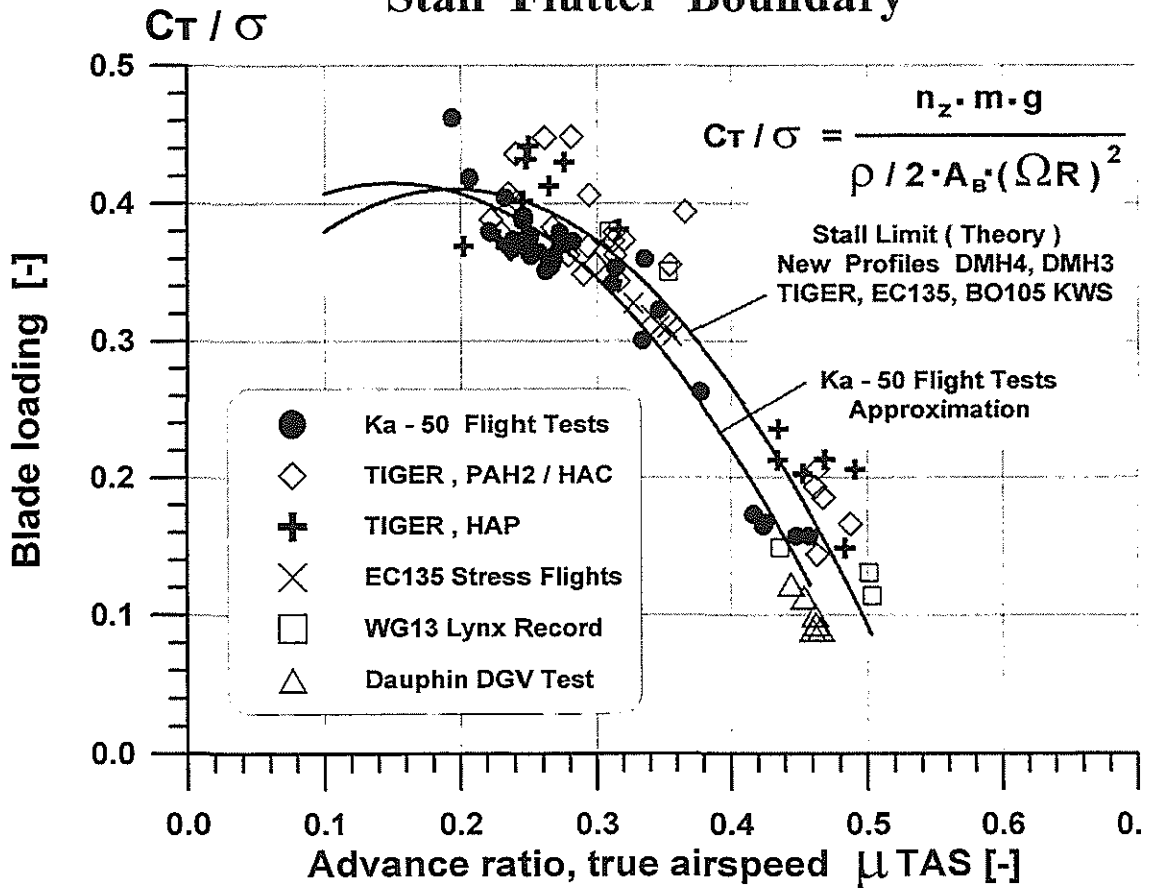


Fig.10

Ka - 25 Helicopter 3ω Vertical Vibrations

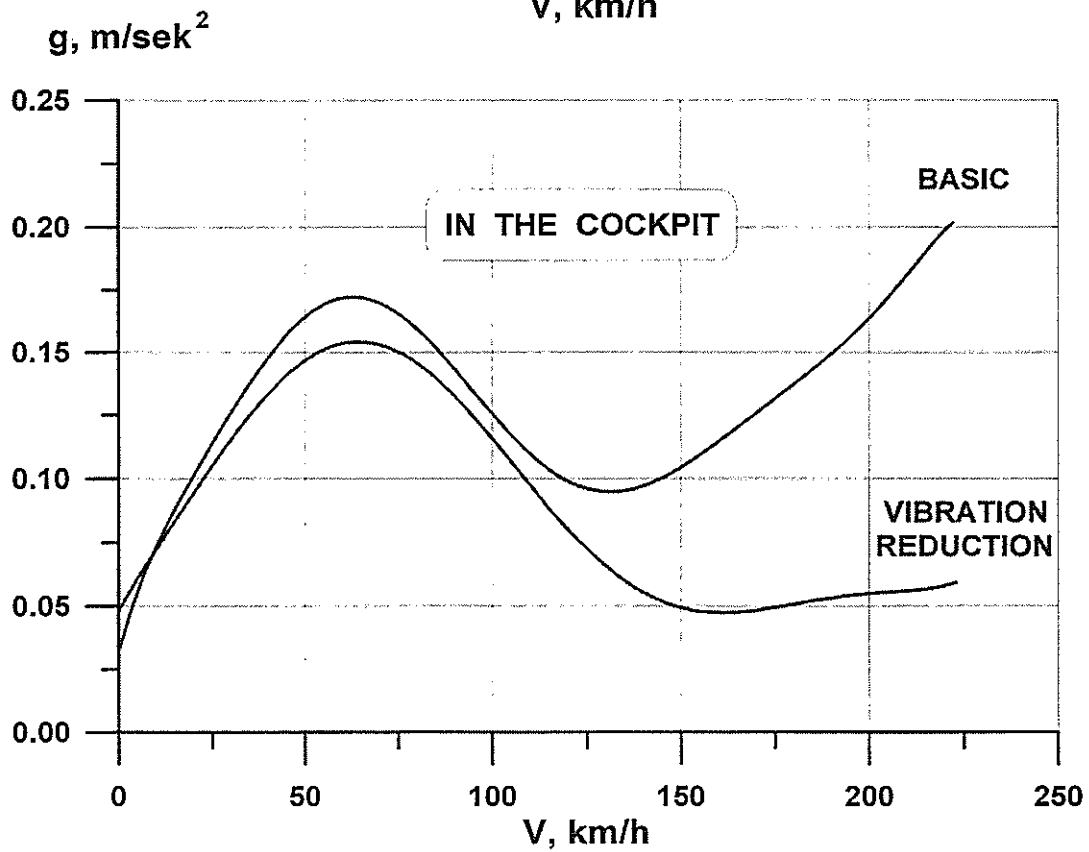
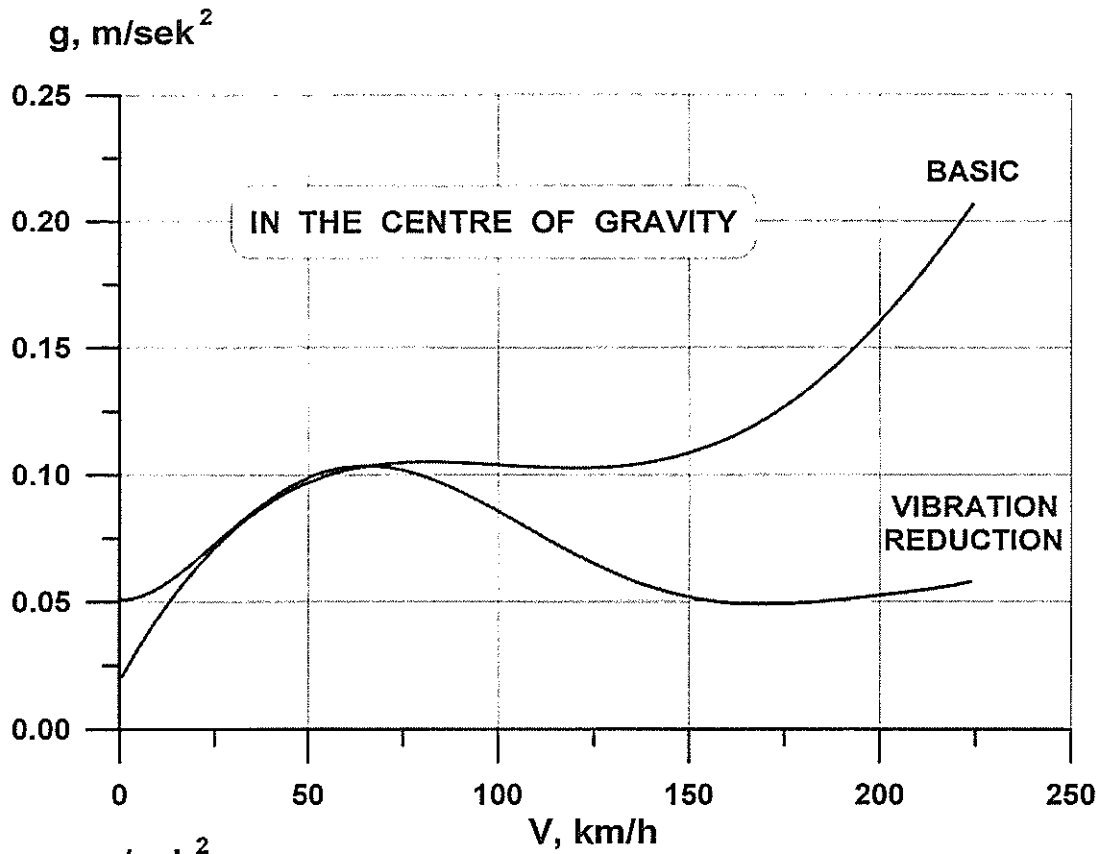
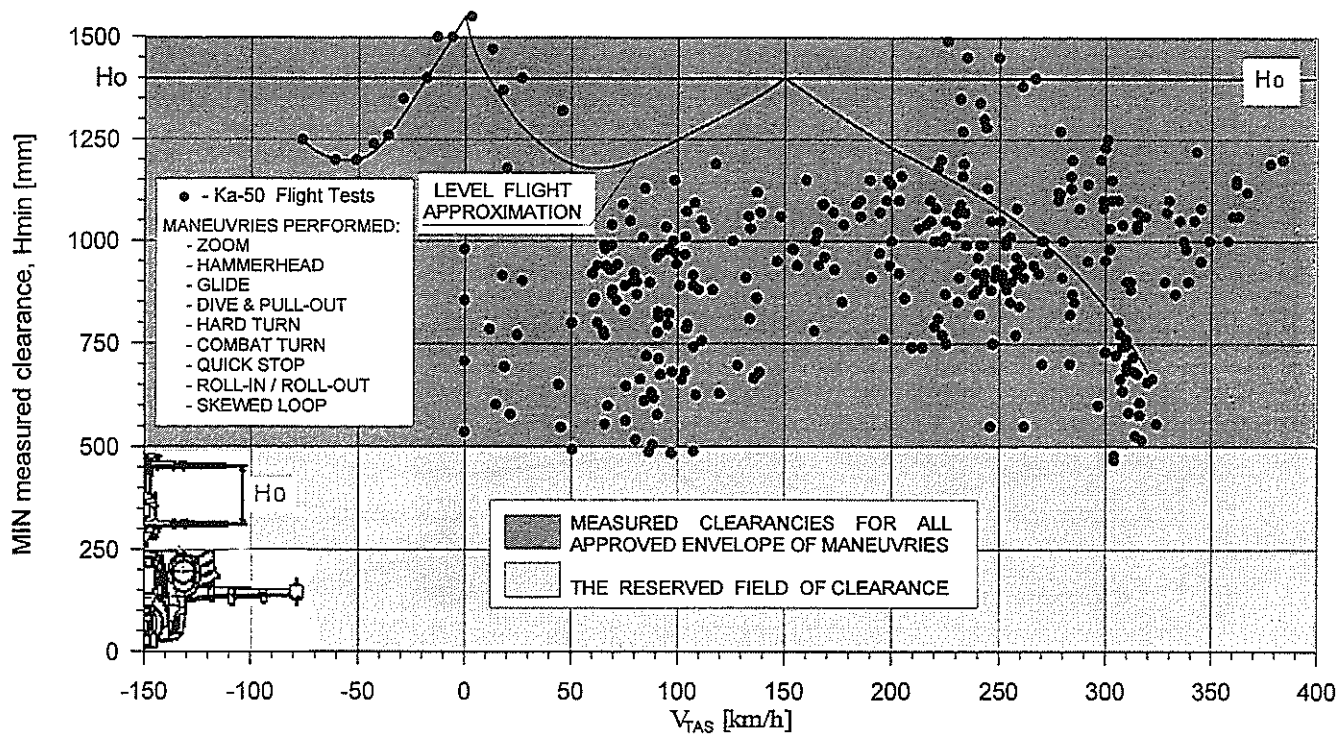


Fig.11

Measured Upper-to-Lower Rotor Blade Tips Clearancies



Load Factor / Speed Envelope (Structural Qualification)

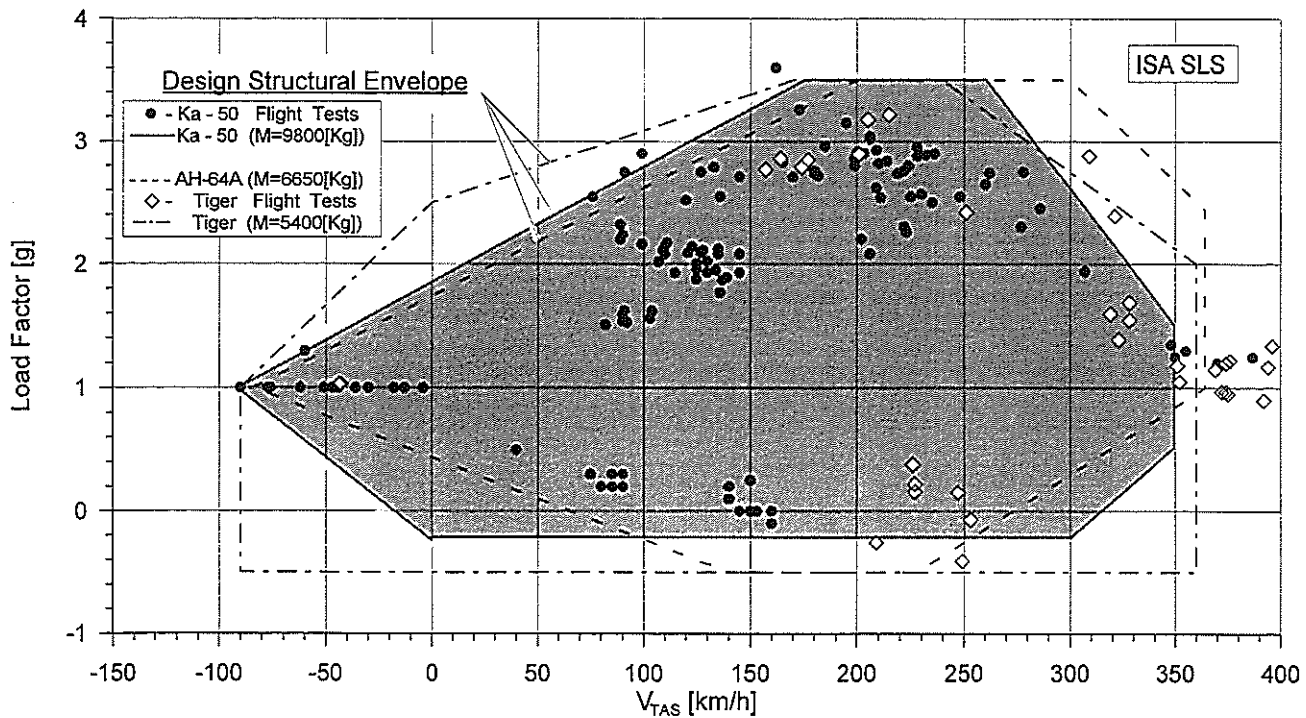


Fig.13

Ka-50 Aerobatic Maneuvres

MANEUVER	The Measured Parameter Values (min/max)				DESCRIPTION
	Airspeed V_{TAS} [km/h]	Load Factor [g]	Pitch attitude [deg]	Roll attitude [deg]	
Hard Turn (Right/Left)	280 ÷ 60	1.0 → 2.9 → 1.0	20 ÷ 50	0 ÷ -70	Unsteady Turn with Pitch & Roll
Flat Turn (Right/Left)	220 ÷ 0	1.0 → 1.5 → 1.0	±5	±20	Jaw Attitude ±80 ÷ ±90 [deg]
Hammerhead (Right/Left)	280 ÷ 0	1.0 → 2.9 → 1.0 → 2.9 → 1.0	0 ÷ ±90	±90	
Dive	0 ÷ 390	1.0 → 0.25 → 2.9 → 1.0	0 ÷ -90	±30	Push-Down, Dive & Pull-Out
Skewed Loop (Right/Left)	280 ÷ 70	1.0 → 2.9 → 1.2 → 3.5 → 1.0	0 ÷ 360	±150	
Quick Stop (Right/Left)	150 ÷ 40	1.0 → 2.0 → 1.2 → 1.0	0 ÷ 40	±55	Pitch / Roll Deceleration
Pull-Up with the Tail Forward	-90 ÷ 0	1.0 → 1.5 → 1.0	0 ÷ -70	±10	Backward Acceleration & Pull-Up with the Tail Forward/Up

Flight Path While Performing Skewed Loop

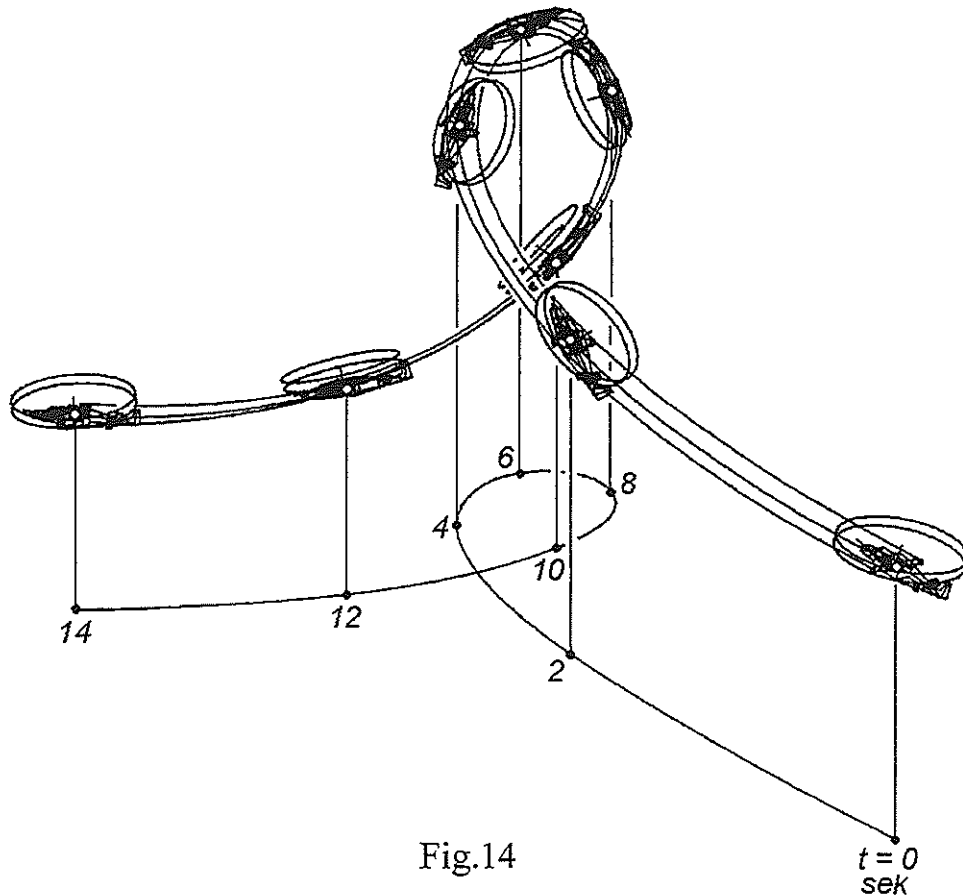


Fig.14